V European Conference on Computational Fluid Dynamics
ECCOMAS CFD 2010
J. C. F. Pereira and A. Sequeira (Eds)
Lisbon, Portugal, 14–17 June 2010

EXPERIMENTAL AND NUMERICAL INVESTIGATIONS OF THE LAMINAR-TURBULENT TRANSITION MECHANISMS IN THE BOUNDARY LAYER ON 2D AND 2.5D MODELS IN THE LOW TURBULENCE WIND TUNNEL

Sergey L. Chernyshev, Alexander I. Ivanov, Andrey Ph. Kiselev, Vladimir A. Kuzminsky, Dmitry S. Sboev and Sergey V. Zhigulev

Central Aerohydrodynamic Institute n. a. prof. N.E. Zhukovsky (TsAGI)
Zhukovsky, Moscow Region, 140180, Russia
e-mail: slc@tsagi.ru, ivanov_a_i@list.ru, a-ph-kiselev@ya.ru, vladimir.kuzminsky@ya.ru, ife@ngs.ru, zhigulevv@mail.ru

Key words: Laminar-turbulent transition, Low-turbulence wind tunnel, Hot-wire anemometer measurements, Tollmien-Schlichting waves, Cross-flow instability, Linear stability transition prediction method

Abstract. *The results of experimental investigations of the influence of free stream turbulence level and acoustic disturbances on laminar-turbulent transition on the airfoil (2D model) and 35° swept wing (2.5D model) are discussed. The experiments were carried out in TsAGI low-turbulence wind tunnel at the flow velocity about 80 m/s. Both models had the same streamwise cross-section (1 m chord LV6 airfoil). To increase initial flow turbulence level, the turbulizing grids were used. All measurements were accomplished using the hot-wire anemometer. The tests show that for natural low-turbulence conditions (ε_u=0.064%) the laminar-turbulent transition is realized near the X/C=0.62 through the instability of the local separation zone with respect to wave packet in the frequency range 1.5-2.5 kHz which appears as a result of transformation of the disturbances in the external flow into Tollmien-Schlichting waves. Under the acoustic influence on the boundary layer in the range 2.0-2.8 kHz and with the level of the noise pressure of 91-108 dB, the laminar-turbulent transition is shifted upstream to X/C=0.55-0.57. At the higher level of turbulence, the laminar-turbulent transition line shifts towards the model leading edge even more sufficiently (e.g. to X/C=0.22-0.24 at ε_u=0.7%). In the case of 2.5D model at low turbulence, the cross-flow instability mechanism dominates and turbulence generation is associated with the development of high-frequency disturbances in the boundary layer with the central frequency of 1.7 kHz resulting from the secondary instability of the cross-flow stationary vortices. The transition line also shifts to the model leading edge with the turbulence rise, but acoustic receptivity of the boundary layer in this case was found to be very week. The stability characteristics of laminar boundary layer under experimental conditions were calculated using the method based on the linear hydrodynamic stability theory. These data were compared with the results of the experimental study.*

1 INTRODUCTION

Investigations on the development of energy-saving and environmentally-friendly technologies in aviation are actively performed at present in Europe and elsewhere. The friction drag reduction is one of the main reserve of fuel economy and decrease in CO_2 emission. The numerous previous investigations have demonstrated effectiveness of aircraft surface laminarization application with the aim of friction drag reduction.

The interest in the laminar flow control problems has revived at present [1]. The inspired results of the laminar flow control at supersonic speeds were obtained [2]. The investigations on the development of passenger sub- and supersonic airplanes with the use of various laminar flow control concepts are carried out under the projects TELFONA, SUPERTRAC and HISAC of the Sixth Framework Program [3].

The major objective of TELFONA is the development of the capability to predict the in-flight performance of a large NLF aircraft using wind tunnel tests and CFD calculations. Initial studies regarding this objective highlighted a number of problems with the procedure used classically for fully turbulent aircraft.

At the design process of aircraft owing to the necessity of models testing at various regimes these tests are implemented not in a one, but in two or more wind tunnels, which differ in integral level and scale of initial turbulence, in turbulence energy spectrum, so as in noise level and acoustic spectrum. The consequence of the reasons mentioned above is the appreciable mismatching of experimental data obtained in different wind tunnels and in the flight.

Two unresolved problems take place: improvement of convergence of experimental data obtained in various wind tunnels and scaling of these data to flight conditions. Usually investigators try to resolve specified problems by transition trips mounting on the model surface, in that way shifting the laminar-turbulent transition location closer to the model nose. However, such approach is unacceptable under development of laminar aircraft, and the problems associated with initial turbulence influence on the flow characteristics and scaling of experimental data to flight conditions is especially acute.

For solution of the above mentioned problems the developer's toolkit is necessary which allows computing the characteristics of boundary layer stability and laminar-turbulent transition with sufficient accuracy for flight conditions as well as for various wind tunnels. At the same time the testing of various boundary layer stability and laminar-turbulent transition prediction methods by comparison of calculation results and experimental data is of great importance. In particular, determination of the dependence of computed values of N-factor corresponding to laminar-turbulent transition at experimental conditions on the initial turbulence level is of great interest.

In the present work the results of experimental investigations of the influence of free stream turbulence level and acoustic disturbances on laminar-turbulent transition on the LV6 airfoil (2D model) and 35º swept wing (2.5D model) obtained recently at TsAGI in the framework of TELFONA Project are discussed. The stability characteristics of laminar boundary layer under experimental conditions were calculated using the method based on the linear hydrodynamic stability theory. These data were compared with the results of the experimental study. The N-factor values corresponding to experimental transition location (N_{tr}) at various free-stream turbulence levels and acoustics disturbances were obtained.

2 EXPERIMENTAL EQUIPMENT AND WIND TUNNEL TESTING TECHNIQUE

2.1 Aerodynamic facility

Tests of LV6 laminar airfoil and swept wing models were targeted at the investigations of the influence of initial turbulence level of the flow and acoustic disturbances on laminar-turbulent transition. The experiments were conducted in TsAGI T-124 wind tunnel.

TsAGI T-124 subsonic wind tunnel (velocity range – V = 2…100 m/s) is a closed-circuit compressor wind tunnel with test section dimensions of 1 m×1 m×4 m [4].

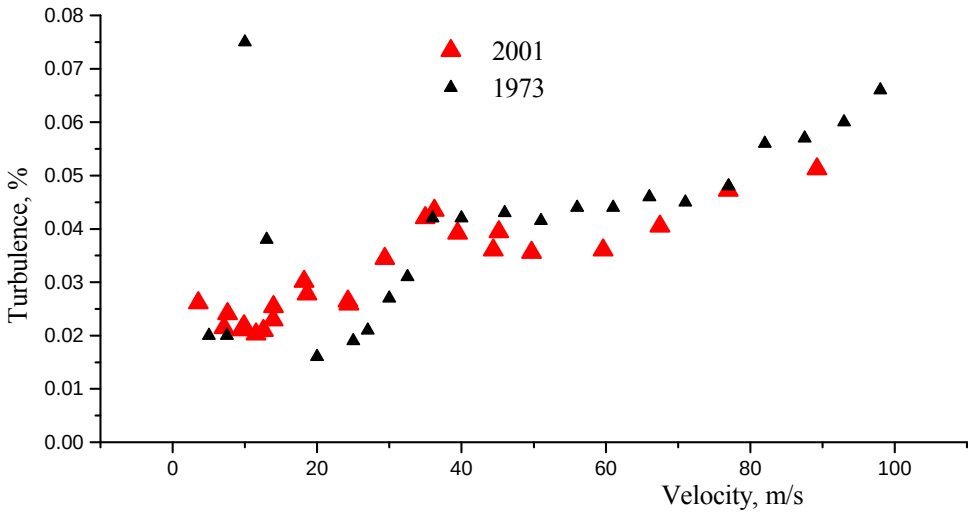

Fig. 1: Initial flow turbulence level in the test section of T-124 TsAGI wind tunnel.

Wind tunnel T-124 is remarkable for sufficiently low initial turbulence level and low noise. These characteristics were achieved by means of applying high contraction ratio in the nozzle (17.6), high accuracy of maintaining the fan speed, using deturbulizing grids in the settling chamber with the inner cell size of 0.7 mm, applying diffuser with a small opening angle, thorough finishing of the inner surfaces of the facility's channels and making of wood almost all basic elements of the wind tunnel with the exception of the test and fan sections. Fig. 1 shows dependence of the initial degree of flow[1] turbulence on the speed, measured at different times. As it is seen, for the flow speed of less than 80 m/s the level of initial turbulence appears to be only 0.05%. It creates favorable conditions for researches of the boundary layers development leading, in the end, to the laminar-turbulent transition.

Since one of the goals of the given research is the investigation of the influence of initial flow turbulence level on the transition, in order to increase it two turbulizing grids were used, which were installed at the point of entry to the test section of the wind tunnel. Both grids have equal wire diameter of 1.5 mm but different cell sizes of 25 mm×25 mm (grid No.1) and 50 mm×50 mm (grid No.2). Both grids have considerably small cell sizes and, at the same time, acceptable level of the test section blockage.

[1] The initial turbulence level of the wind tunnel is measured in the flow core at the point of entry to the empty test section.

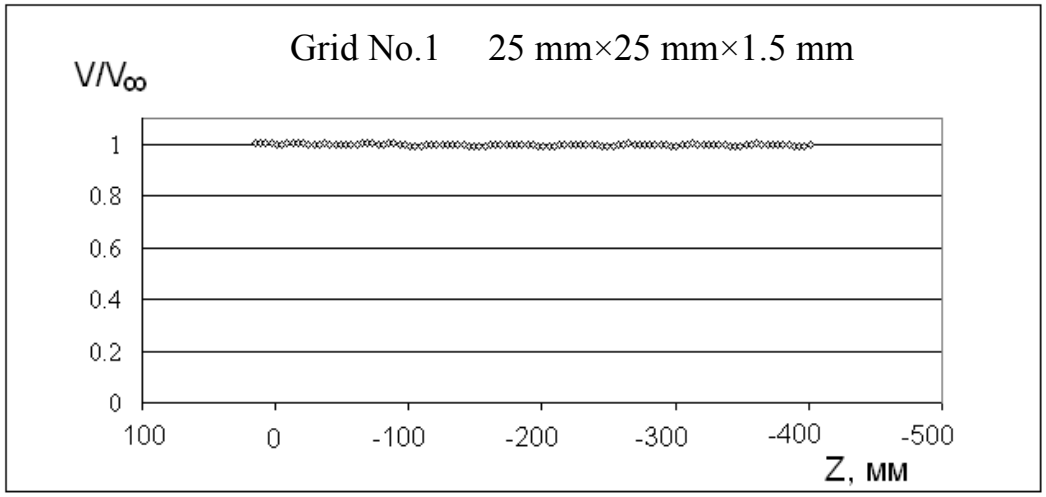

Fig.2: The average velocity field downstream of the grid 25mm×25mm×1.5mm.

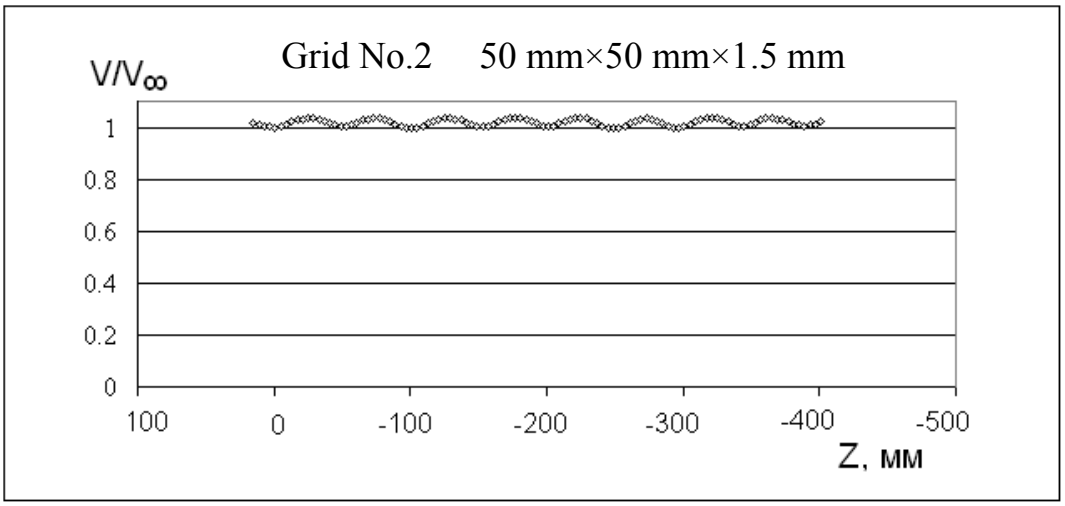

Fig. 3: The average velocity field downstream of the grid 50mm×50mm×1.5mm.

The nature of the flow downstream of these grids was investigated in details in the empty test section. Figures 2 and 3 show results of the pneumometric measurements of the average flow field downstream of both grids at the distance approximately corresponding to the model leading edge position (Z is the distance from the test section longitudinal axis in lateral direction). It is seen, that the flow downstream of the grid 25 mm×25 mm×1.5 mm is almost homogeneous. The homogeneity of the average flow downstream of the grid 50 mm×50 mm×1.5 mm is noticeably worse – the wake structures behind the grid wires can be observed.

The results of the hot-wire measurements of the longitudinal average velocity field, root-mean square values of the velocity fluctuation $\sqrt{<u'^2>}, \sqrt{<v'^2>}$ and correlation $<u'v'>$ are shown in the Fig. 4. It is seen that in the same way as the average velocity, the fluctuation characteristics are subject to periodic changes with the typical spatial scale approximately equal to the size of the grid cell. The results of the average velocity measurements, both pneumometric and hot-wire ones, evidence that the non-homogeneity of the field in the form of the maximal deviation from the mean value is

not larger than ±0.5% for the grid 25 mm×25 mm×1.5 mm and ±1.0% for the grid 50 mm×50 mm×1.5 mm. The root-mean-square (rms) values of the velocity fluctuation are equal to: longitudinal $<\sqrt{<u'^2>}>$=0.59%, lateral $<\sqrt{<v'^2>}>$=0.46% for the first grid (No.1). For the grid with larger cells (No.2) the corresponding values are 0.91% and 0.67%.

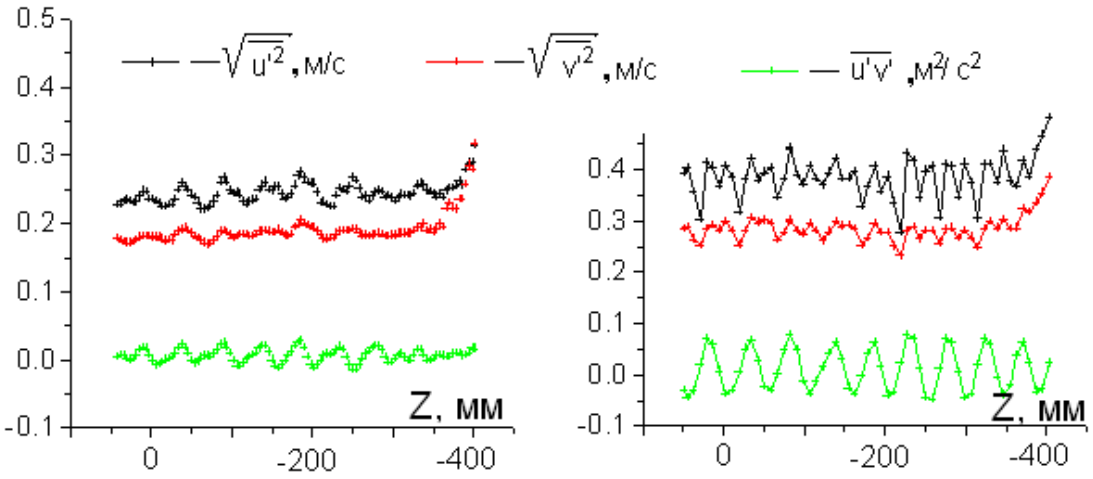

Fig. 4: The field of average velocity and fluctuations at the distance 2400 mm downstream of the grids 25mm×25mm×1.5mm (on the left) and 50mm×50mm×1.5mm (on the right).

Additional measurements with the use of single-wire sensor of constant temperature anemometer (CTA) at a distance of 730 mm ahead of the model mounted in the wind tunnel test section showed that downstream of the grid No.1 turbulence level ε_u was 1.26 %, and downstream of the grid No.2 – 1.5 %. At the model leading edge turbulence level may be estimated by the values ε_u of 0.6-0.7 % for grid No.1 and 1.0-1.1 % for grid No.2. Estimation of the longitudinal integral turbulence scale Λ was made by means of integration of the autocorrelation function. For grid No.1 the value of this scale at a distance of 730 mm upstream of the model was 21.3 mm, and for grid No.2 – 44.7 mm. The Taylor micro-scale of turbulence λ for the longitudinal pulsations was also estimated from the autocorrelation function in a standard way. Its value appeared to be equal to 5-6 mm for both grids. The values of the pressure recovery coefficient for these grids were 0.90 and 0.96, correspondingly.

Acoustic disturbances were introduced into the flow by the dynamic loudspeaker with peak power of 50 W, installed in the test section window of the wind tunnel upstream of the model. The accuracy of the reproduction by the loudspeaker of the sound generator signal frequency was not worse than 0.1 Hz. During the measurement process, special attention was paid to the settling chamber temperature control, because this parameter strongly influences the characteristics of the acoustic waves introduced into the flow. The obtained values of sound pressure appeared to be in the range 91-108 dB.

The hardware component of the measuring system used in the given research consisted of container for 32 pressure sensors of the ТДМ4 type and the constant temperature anemometer of the DISA 55D01 type with a sensor. In order to move the hot-wire in the boundary layer near LV6 airfoil and swept wing models surface the compound coordinate mechanism was used, which includes the basic *XZ*-traverse gear and installed on it automated *Y*-traverse gear. The *Y*-traverse gear was connected to the

PC through the input-output subsystem. The step size in the direction normal to model surface of the *Y* traverse gear was equal to 0.01mm.

2.2 Models description

LV6 airfoil model is a rectangular wing with the chord of 1000 mm and the span of 998 mm. The shape of the laminarized airfoil is close to symmetric one; its outline is shown in Fig. 5. The model is placed in the closed test section of the wind tunnel T-124 from wall to wall at the equal distances from the floor and from the ceiling. Since with such position of the wing there is no tip vortices, the modeling of the flow over the "infinite span" wing is performed in the best way and the flow in the middle may be considered as two-dimensional.

Fig. 5: Outline of the LV6 airfoil.

The second model has been tested is the wing section model with the sweep angle $\chi = 35^{o}$, with the chord length along the free stream direction $C = 1000$ mm and the span of 998 mm. This model has the same shape of the LV6 laminarized airfoil in the section along free stream direction, with the relative thickness of 11%.

In the closed test section of the T-124 wind tunnel the swept wing model was also placed at the equal distances from the floor and from the ceiling from wall to wall. For prevention of the spreading additional disturbances along leading edge from the junction area of the wing and right side (in stream direction) test section wall, the model was equipped with the fence. The fence was fixed at distance of 120 mm from the right wall of the test section

In the tests a task was posed to study the transition mechanism associated with the Tollmien-Schlichting waves or cross-flow instability development in the 2D flow or infinite swept wing condition. Before the main tests, it was necessary to make certain that in the central part of the models there are areas in which the flow parameters do not depend on the lateral coordinate *Z*. For this purpose both models were equipped with three rows of pressure taps.

3 STABILITY CALCULATIONS

The calculation of laminar boundary layer was conducted using the algorithm and computer code [5], which are based on finite-differences scheme of second order accuracy of approximation along longitudinal coordinate and fourth order accuracy along coordinate normal to the surface [6]. In calculations the experimental pressure distributions were used.

General numerical matrix method for calculation of hydrodynamic stability characteristics of three-dimensional boundary layers [7] developed in TsAGI was used in the present work. According to method [7], the computation of eigenvalues was performed for real counterpart of initial complex matrix with the use of QR-algorithm. This method was tested for yawed wing and flat plate boundary layer flows by means of comparison with the experimental data [8, 9] and with the results of calculations by eigen function orthogonalization method [10] within the range of upstream Mach number $0.2 \leq M \leq 4.5$.

4 2D RESULTS

4.1 Natural conditions

The experiments were conducted at velocities of the flow 80 m/s that corresponds to Reynolds number $Re_\infty = 5.5\times10^6$ based on the model chord and Mach number $M_\infty = 0.24$. All measurements with the 2D model were performed at $\alpha = 0^o$ on the upper surface within the range $X/C = 0.2\ldots0.7$ by means of single-wire sensor of CTA.

Measurements of pressure distributions on the both upper and lower surfaces of the LV6 airfoil model have shown that in the investigated range of angles of attack pressure distributions in three sections practically coincided and flow with good accuracy may be considered as two-dimensional. An example of comparison of pressure distributions along X-axis (X=0 at the leading edge of the model) for α=0° is shown in Fig. 6.

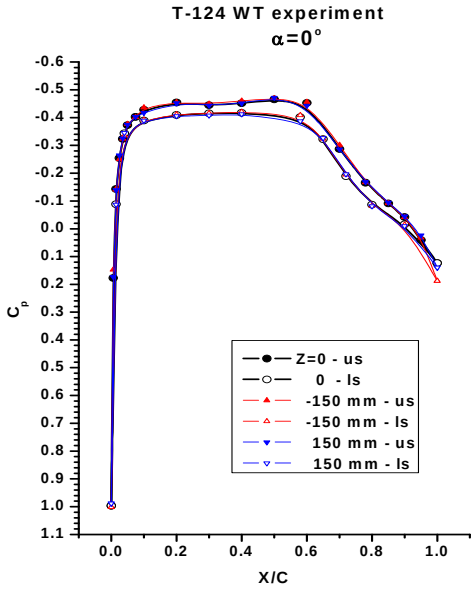

Fig. 6: Chord-wise pressure distributions on upper and lower surfaces of the LV6 airfoil at α=0º at different span sections

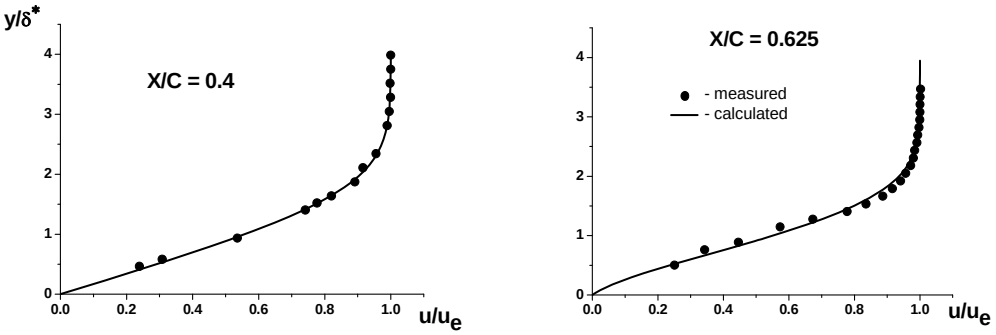

Fig.7: Calculated and measured velocity profiles in the laminar boundary layer at the middle section on upper surface of the LV6 airfoil model ($\chi = 0^o$) under T-124 wind tunnel experimental condition.

Fig. 7 shows the calculated profiles of mean velocity in the boundary layer in comparison with hot-wire data. The evolution of profiles is seen from the laminar

profile at *X/C* = 0.4 till the velocity profile with the inflection point at *X/C* = 0.625. As seen from this figure, as well as from downstream development of boundary layer displacement and momentum thicknesses (Fig. 8), the results of boundary layer computations are in rather well agreement with the experimental data. The obtained results in natural conditions evidence that in the area *X/C* = 0.60-0.65 on the model the separation bubble was developing.

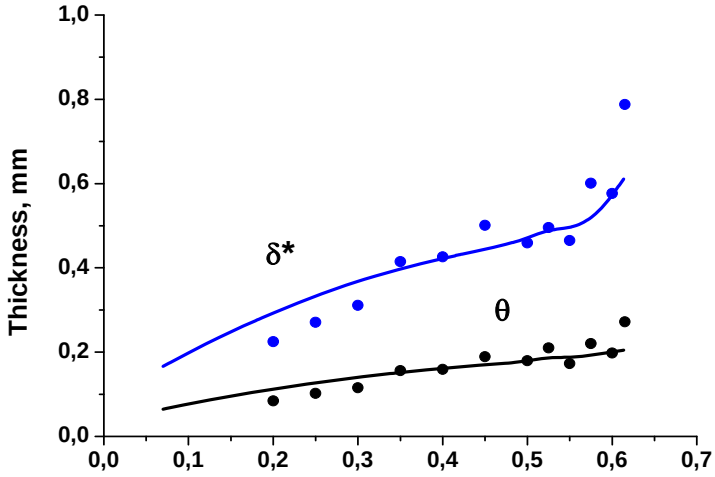

Fig. 8: Calculated and measured displacement δ* and momentum θ thicknesses at the middle section on upper surface of the LV6 airfoil model (χ = 0°) under T-124 wind tunnel experimental conditions.

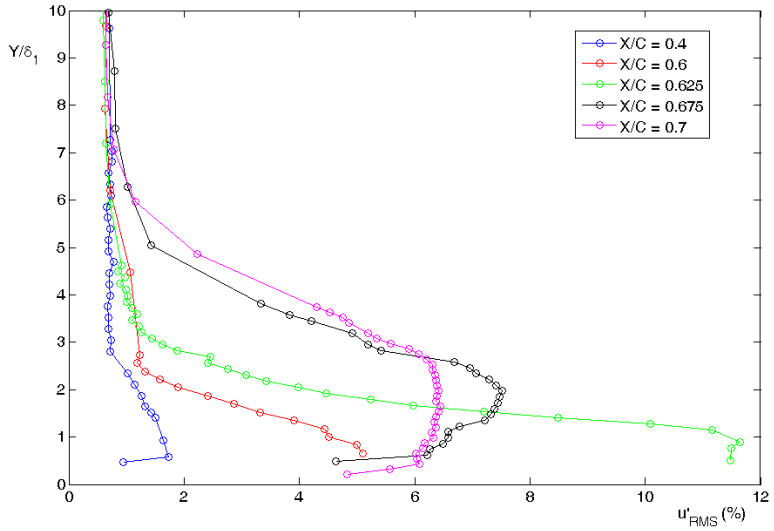

Fig.9: The profiles of integral (over the spectrum) pulsations of the longitudinal velocity component for different *X/C* values.

The profiles of integral (over the spectrum) pulsations of the longitudinal velocity component for different *X/C* values and the frequency spectra of disturbances measured in the boundary layer are shown in Figs. 9 and 10. The spectra in the subsequent points *X/C* in the downstream direction are shifted by the decade each. Analysis of spectra show that the disturbances forming the packet with central frequency near 2.1 kHz are growing in the boundary layer and that the frequency of the most unstable disturbances

decreases downstream. The chord-wise distributions of calculated and experimental values of frequencies of the most quickly growing disturbances are presented in Fig. 11. As seen from this figure, the results of computations based on linear hydrodynamic stability theory are in reasonable agreement with the experimental data. From this data and wall-normal profiles of different spectral components its can be concluded that this disturbances are Tollmien-Schlichting (TS) waves. In present set-up the generation of TS waves occurs due to uncontrolled external acoustic disturbances. In natural conditions growth of TS waves appears to be linear up to downstream position X/C=0.6.

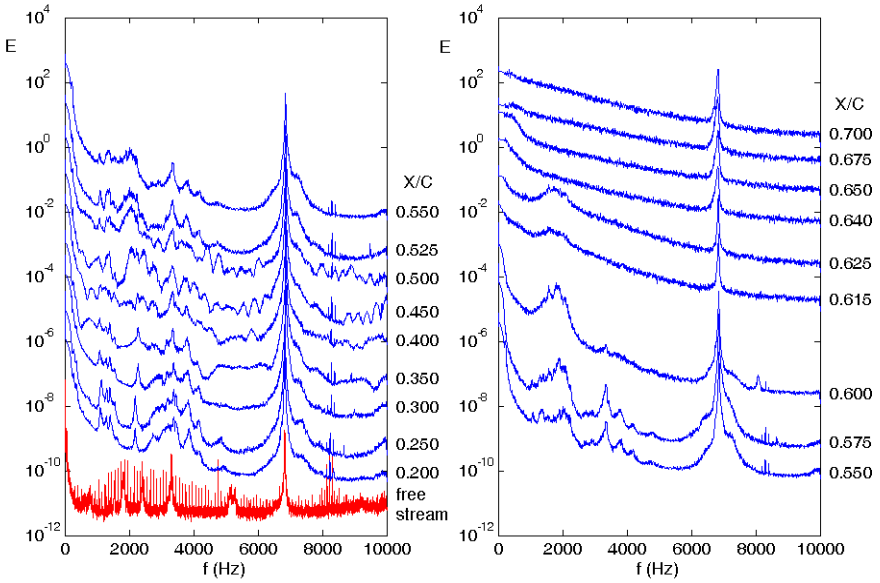

Fig.10: The pulsation spectra measured in the boundary layer along the line of constant mean velocity U/U_e=0.55.

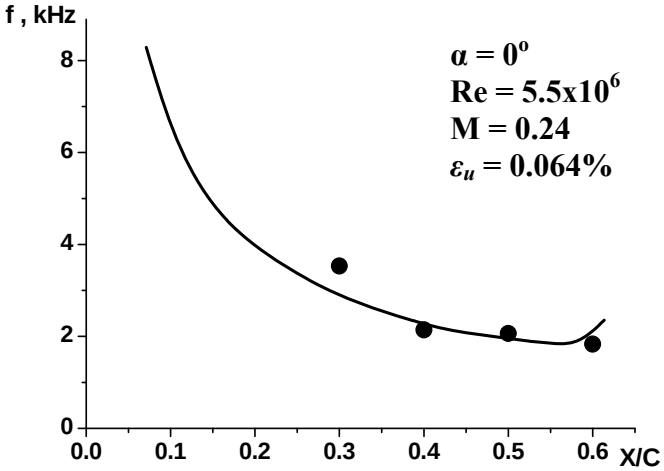

Fig.11: Chord-wise distribution of calculated and measured frequencies of most quickly rising disturbances on upper surface of LV6 profile model at T-124 wind tunnel test conditions.

Fig. 12 shows dependence on streamwise coordinate of the rms amplitude of integral pulsations and the amplitude of disturbances in different frequency ranges measured in boundary layer along the line $U = const$. Low-frequency disturbances in the band 0-

300 Hz, corresponding to the so-called Klebanoff modes, make principal contribution to the pulsation energy up to $X/C = 0.6$. High-frequency acoustic disturbances do not influence the laminar-turbulent transition in the natural conditions. The rise of disturbances in the frequency band 5-10 kHz is caused by filling of the high-frequency part of spectrum in the process of laminar flow destruction.

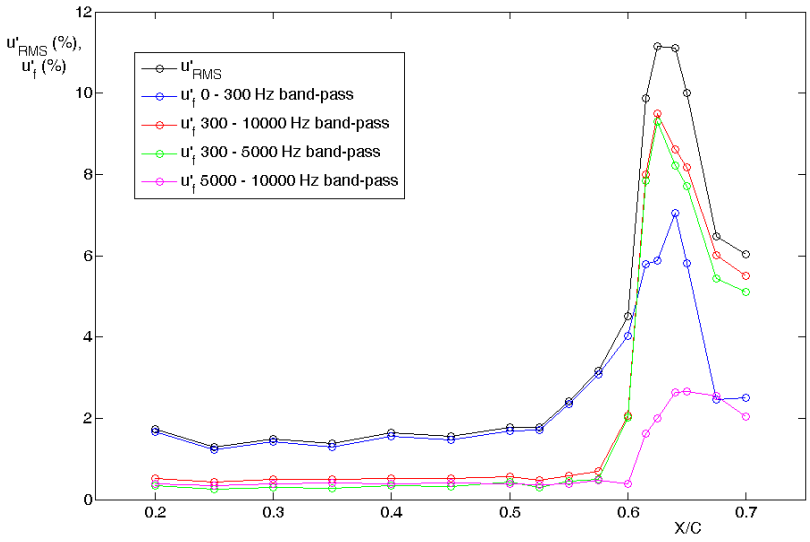

Fig.12: Curves of increase of the rms amplitude of the integral pulsations and the curves of increase of disturbances in different frequency ranges along the line U/U_e=0.55.

Fig. 12 shows that the laminar-turbulent transition process is caused by the sharp rise of disturbances in the frequency range 0.3-5 kHz in the zone X/C = 0.600-0.615. This corresponds to instability of the local separation zone. The appearance of this instability is connected with transformation of the above described packet of the TS waves with central frequency near 2.0-2.1 kHz into the disturbances of separated flow. In the pulsation spectra this packet is observed up to X/C=0.625, i.e. to the latest phases of laminar-turbulent transition when intensive filling of the high-frequency part of spectrum takes place. As it follows from Fig. 11, the maximum of the curve of rms amplitude integral pulsations is located between X/C=0.615 and 0.625. This region defines the location of the laminar-turbulent transition region at the given flow regime.

4.2 Influence of artificially excited acoustic disturbances

The measurements were accomplished at frequencies of the sound between 1200 and 3000 Hz. For the frequency f_s = 2000 Hz the measurements were performed with values of sound pressure p'_s = 108 dB and p'_s = 98 dB, although the results for these two cases appeared to be rather close. The data obtained allows to draw a conclusion that for the exciting frequencies 1200 and 1400 Hz in the region X/C = 0.2-0.6 boundary layer remained laminar. For the frequencies in the range 1600-1900 Hz the non-linear development of the TS waves was observed, but to X/C = 0.6 turbulent condition of the boundary layer was not yet achieved. The results obtained allow to affirm that the N-regime of the laminar-turbulent transition in the boundary layer is observed [11]. As it is known, this regime is characterized by the resonance excitation of the low-frequency oscillations (see Fig. 13), with the absence of influence of subharmonics on the main wave at the early stages (stages of the parametric resonance). Laminar-turbulent transition was fixed for the frequencies of the excitation exceeding or equal to 2000 Hz in the region X/C = 0.550-0.575, i.e. upstream of the separation bubble observed in the

natural conditions. The data obtained force to suppose that in the exciting frequency range from 2000 to 2800 Hz the transition location shifts upstream with the rise of the acoustic wave frequency, but this shift is not large and in all cases boundary layer at $X/C = 0.55$ remained laminar.

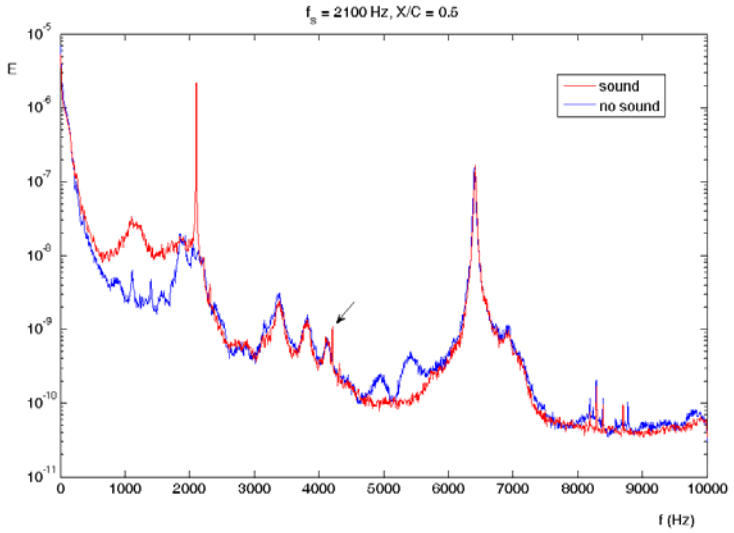

Fig. 13: The resonance excitation of the low-frequency oscillations.

4.3 Influence of free-stream turbulence level

The curves of amplification of integral pulsations measured in the boundary layer with the turbulizing grids, which are installed at the point of entry to the test section of the wind tunnel are shown in Fig. 14. These curves were obtained as a result of the hot-wire motion along the constant mean velocity $U/U_e = 0.6$ line. Measurements were performed in the range from $X/C = 0.12$ (extreme forward position of the traverse) to $X/C = 0.40$. Relying on the maximum of the amplification curve for grid No.1, position of the laminar-turbulent transition may be localized inside the interval of $X/C = 0.22$-0.24. For grid No.2 it was impossible to determine the maximum of the amplification curve, because it is located upstream of the most forward position of the gauge.

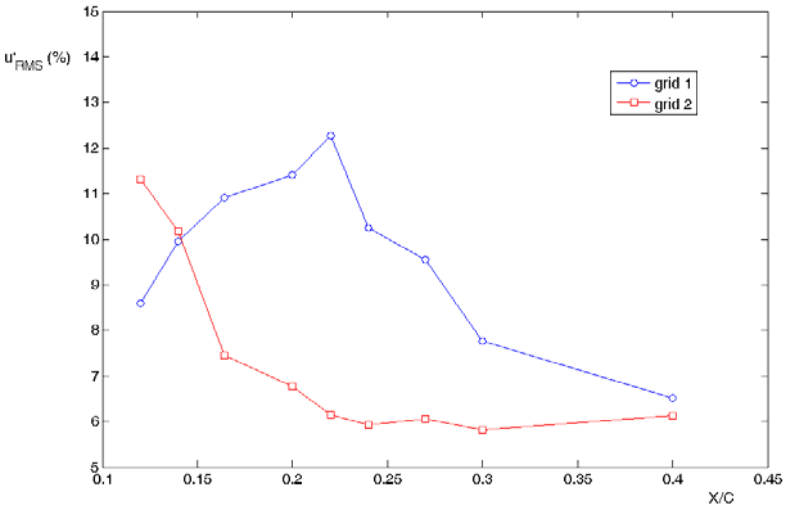

Fig. 14: The curves of amplification of integral pulsations in the boundary layer with the turbulizing grids.

Thus, when the airfoil was tested in the flow with higher level of turbulence, laminar-turbulent transition line shifts towards the model leading edge. This shift becomes more sufficient with the rise of the turbulence level.

4.4 Summary of 2D results

The correlation of N-factor distribution calculated at the middle-span section on upper surface of the LV6 airfoil model with the measured transition locations at the described above experimental conditions for 2D case is presented in Fig. 15.

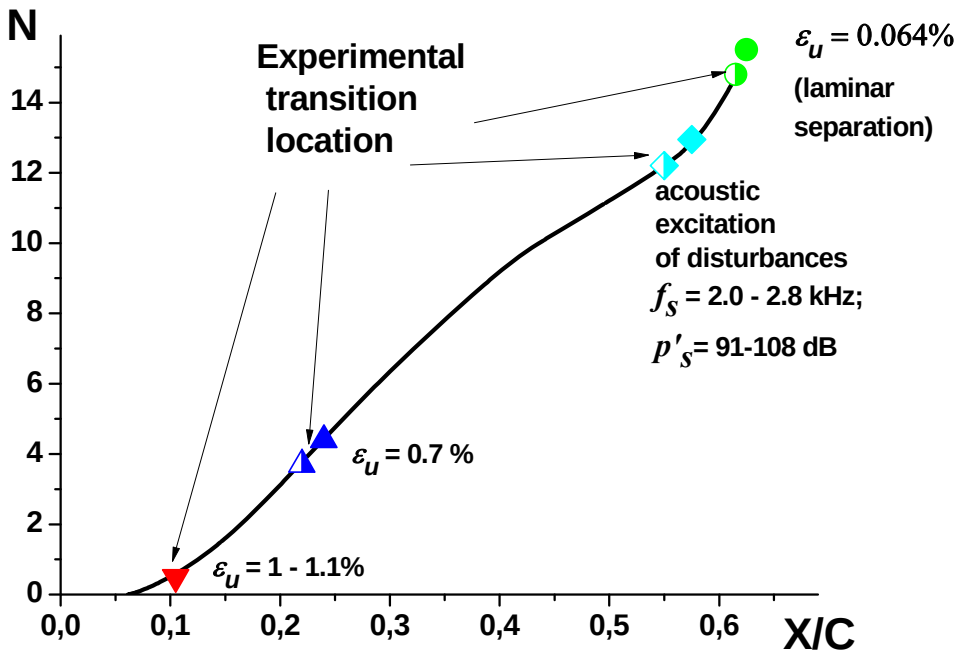

Fig. 15: The correlation of N-factor distribution calculated at the middle-span section on upper surface of the LV6 airfoil model with the measured transition locations at various experimental conditions (semi-bold symbols – transition onset; bold symbols – end of transition).

5 2.5D RESULTS

5.1 Natural conditions

All measurements done in this series of experiments were performed at the incoming flow velocity of 77.4 m/sec. Before the hot-wire measurements, the pressure distributions over the model surface were also measured in the range of effective angles of attack α' from -2.5º to 2.5º with the step of 0.5º.

Pressure distributions obtained at zero incidence demonstrate well-known peculiarities for the upper surface flow on the swept wings with low aspect ratio with wall interference effect. It is seen that in the section I disposed closer to the wing root the minimum of pressure shifts to the trailing edge and in the most distant from the root section III the rarefaction peak shifts to the leading edge.

Pressure coefficient distributions in different sections at α' = -2º coincide much better (Fig. 16). Thus the conclusion may be drawn that for this region of the model span the constant pressure lines are near to parallel to the leading edge and consequently the condition of the wing yawing (2.5D flow) is satisfied. The negative pressure gradient

area at $\alpha' = -2^o$ stretches to $X/C = 0.5$, so it may be concluded that for this angle of attack cross-flow in the boundary layer is more. For this reason regime $\alpha' = -2^o$ was chosen for further investigations.

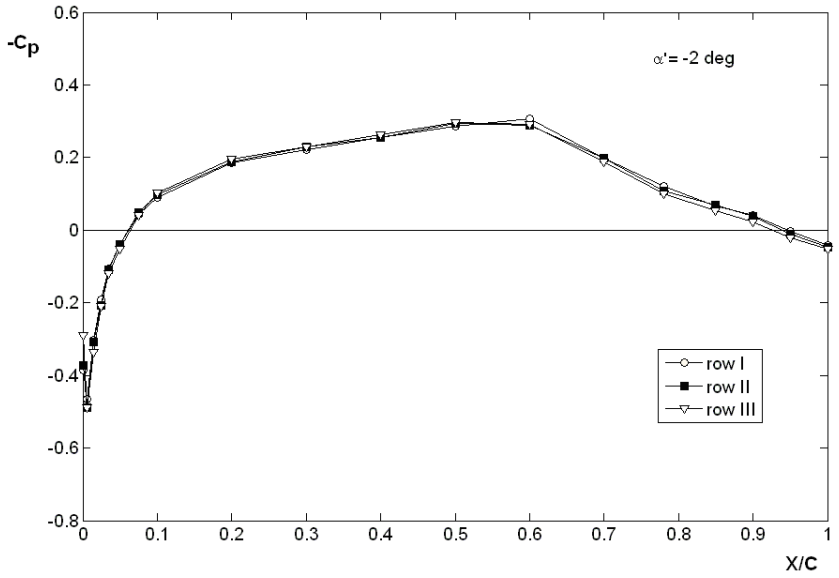

Fig. 16. Pressure distributions on the upper surfaces of the LV6 wing model ($\chi = 35^o$) measured at various span-wise section at $\alpha' = -2^o$.

The flow over the swept wing is subjected to the cross-flow instability caused by the excitation of both stationary and non-stationary cross-flow waves, which are the eigen solutions of the linear stability theory. Development and interaction of these waves result in the laminar-turbulent transition. The complete theory of this process doesn't exist now.

The special investigation of evolution of stationary and traveling cross-flow disturbances was not planned in the present work. The means and methods of measurements chosen for this study do not allow investigating the stationary disturbances in the 2.5D boundary layer case. At the same time, the non-stationary disturbances characteristics registered by hot-wire in such boundary layer, in particular, its frequency composition and reference amplitude, reflect the real physical processes completely enough and allow to define the laminar-turbulent transition location. The investigation of the non-stationary disturbances in the boundary layer is the main method used in the present study. Destruction of the laminar regime is accompanied by increase of the duration of the signal parts including high-frequency pulsations of large amplitude, and their further junction into turbulent signal.

For determination of the laminar-turbulent transition location in boundary layer on the swept wing model the intermittency function γ was used. The intermittency function behavior drastically changes in the transitional area, allowing localizing transition with confidence. In the ref. [12], the value of $\gamma = 0.5$ was used as the transition criterion, but in the present study application of this criterion is not convenient, because it does not allow to compare the results obtained at higher level of the flow turbulence. So the value of $\gamma = 0.8$ was chosen as a criterion of laminar-turbulent transition, corresponding practically to the developed turbulent flow (Fig. 17).

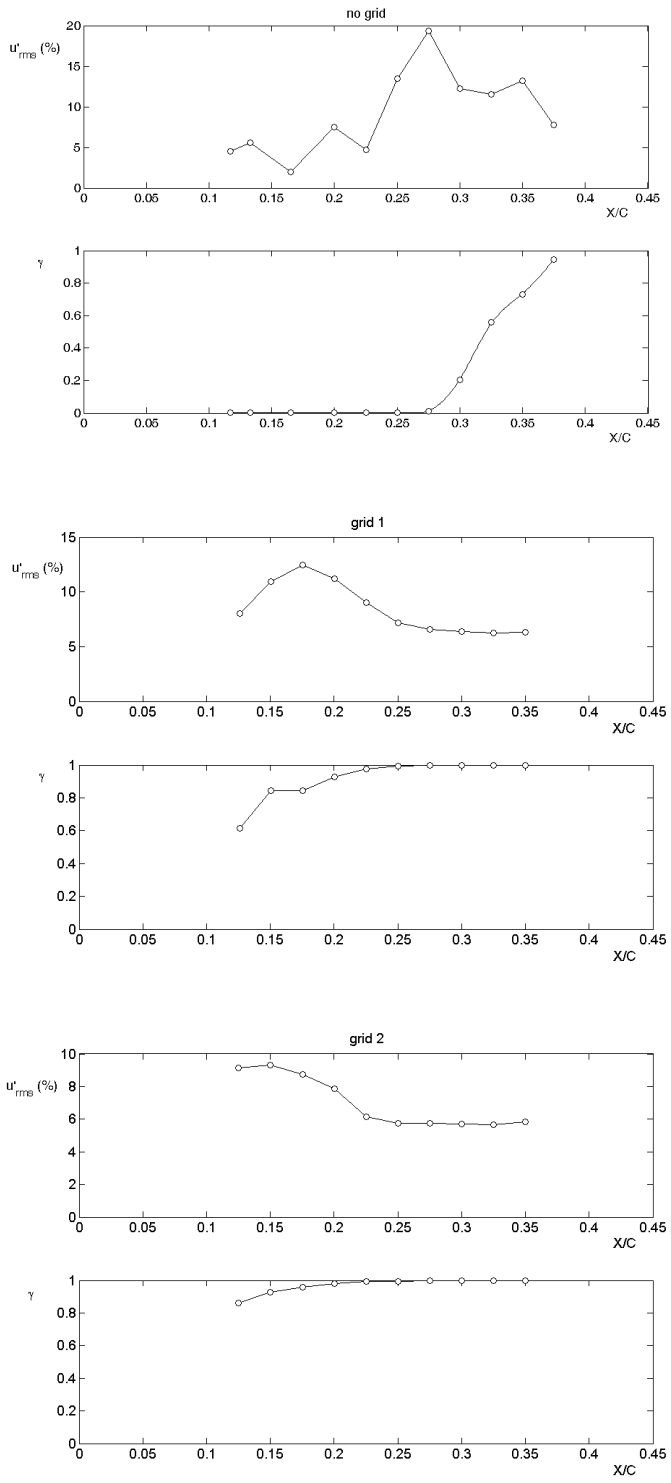

Fig. 17: Downstream development of the u'_{rms} (top) and intermittency γ (bottom) for a fixed altitude in the boundary layer ($U^*/U_e = 0.7$):
a) natural conditions, b) grid No.1, c) grid No.2.

In natural conditions one of the features of the boundary layer flow evolution in our experiments was the appearance of the disturbance packet in the band of 1.0-1.5 kHz downstream from $X/C = 0.133$ (see Fig.18). These disturbances may be identified as non-stationary waves of the cross-flow instability.

Fig. 18 presents comparison of the experimental data with the results of matrix method [7] of 3D boundary layer stability calculations for experimental conditions.

These results are presented in the form of dependence between the frequency of the most unstable disturbance and longitudinal coordinate. The experimental data are given in the form of range of the amplifying frequencies and several values of the most amplified frequencies which were possible to define using the amplification coefficient correlations.

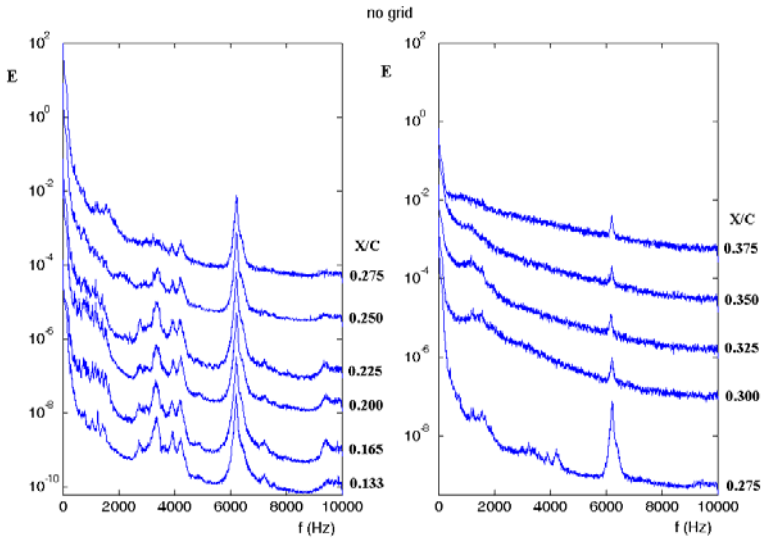

Fig. 18: Energy density spectra of u' for a fixed altitude in the boundary layer ($U^*/U_e = 0.7$), natural conditions. Each successive curve is shifted by decade.

There is rather good qualitative agreement between the theoretical and experimental results. In particular, the reduction of frequencies of the most quickly rising disturbances in the downstream direction is evident. At $X/C = 0.225$ there is also good quantitative coincidence of the results. For the values of longitudinal coordinate higher than $X/C = 0.225$ it was not possible to define frequency of the most quickly rising disturbances from measurements, because due to the diminishing of these frequencies (with the character values about hundreds Hz) their spectral area closes up with the low-frequency disturbances area (character frequencies about tens Hz).

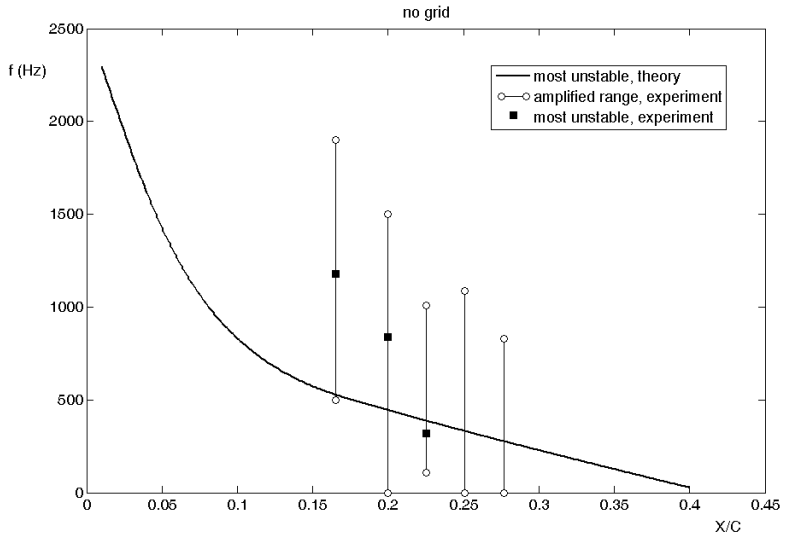

Fig. 19. Comparison between measured and predicted frequencies of the most unstable disturbances at the different X/C, natural conditions.

The appearance of turbulence at this regime is directly associated with the development of the high-frequency disturbance packet with central frequency of 1.7-2.0 kHz in the boundary layer as a result of secondary instability of the stationary vortices in the cross-flow.

Introduction of acoustic disturbances into the flow does not lead to any changes in the disturbance spectra: acoustic peaks simply superpose on the spectrum of disturbances developing in the boundary layer, not changing their structure. The results obtained demonstrate very week receptivity of the 3D boundary layer to acoustic disturbances of external flow and fully identical to the results of ref. [12].

The experiments with the high-turbulence incoming flow showed that the location of the laminar-turbulent transition shifted to the model leading edge. Again the non-linear stages of by-pass transition were observed.

5.2 2.5D results summary

The correlation of N-factor distribution at the middle-span section on upper surface of the LV6 swept wing model calculated by the linear stability theory method [3] with the measured transition locations at the described above experimental conditions is presented in Fig. 20.

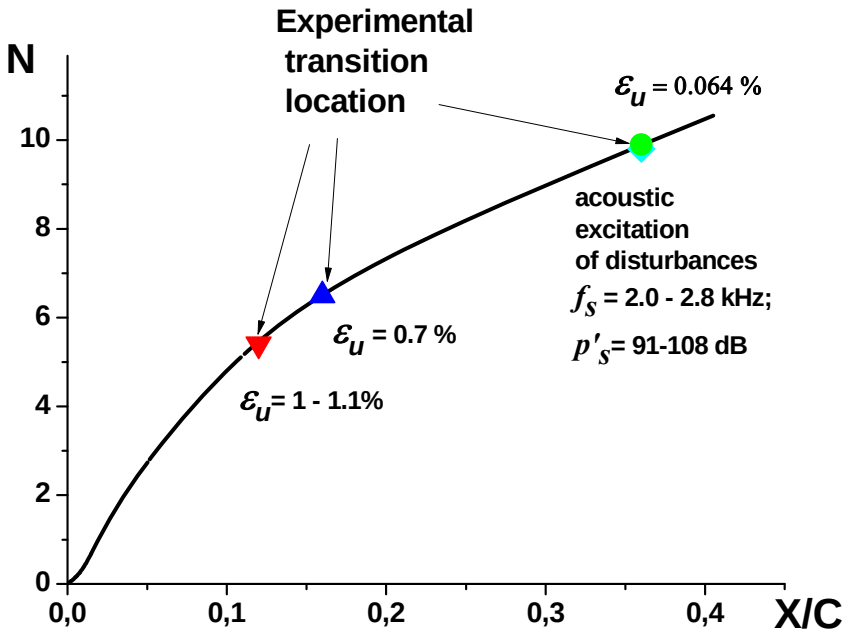

Fig. 20: The correlation of N-factor distribution calculated at the middle-span section on upper surface of the LV6 swept wing model with the measured transition locations at various experimental conditions.

6 CONCLUSIONS

- The stability characteristics of laminar boundary layers on LV6 airfoil and swept wing models under TsAGI T-124 wind tunnel experimental conditions are calculated on the base of linear stability transition prediction method. These results are in reasonable agreement with the obtained experimental data.
- The N-factor values corresponding to experimental transition location (N_{tr}) at various free-stream turbulence levels and acoustics disturbances are obtained.

- The experiments with the higher-turbulence incoming flow showed that values of N_{tr} sufficiently decrease with the rise of the turbulence level both for LV6 airfoil and swept wing models.
- Excitation of acoustic disturbances leads to some decrease in N_{tr} values for 2D boundary layer on LV6 airfoil model. At the same time acoustic influence on the N_{tr} values for LV6 swept wing model in the cases, when the laminar-turbulent transition is caused by cross-flow instability was found to be very weak.
- The e^N-method rather successfully correlates with laminar-turbulent transition. However, the values of N-factor corresponding to transition are substantially different for various external conditions and for various types of instability

7 ACKNOWLEDGEMENT

This work was carried out within TELFONA Project, funded by the 6th European Framework Program.

REFERENCES

[1] H. Bieler, A. Abbas, J.-Y. Chiaramonte and D. Sawyers, Flow control for aircraft performance enhancements. Overview of Airbus – University cooperation. *AIAA paper* nº2006-3692 (2006)

[2] R.D. Joslin, Aircraft laminar flow control. *Annu. Rev. Fluid Mech.* **Vol. 30**, pp.1-29, (1998)

[3] Aeronautics research 2003-2006 projects. Project synopses, *European Commission, Belgium, Luxembourg*, **Vol. 1** (2006)

[4] V.M. Filippov, Characteristics of fluctuations in flow through low-turdulence arerodynamic wind tunnel T-124 designed for small speeds. *Uchenye Zapiski TsAGI.* **Vol. 39**, nº1-2, pp.68-80 (2008) - *in Russian*

[5] V.I. Shalaev, Space-efficient method of numerical solution of turbulent boundary layer equations. *Trudy TsAGI*. Vyp. 2265, pp. 113-124 (1985) - *in Russian*

[6] I.V. Petukhov, Numerical calculation of two-dimensional flow in boundary layer. *Numerical methods of solution of differential and integral and equations and quadrature formulas. Addendum to Journal of Computational Mathematics and Mathematical Physics, Moscow: Nauka*. **Vol.4**, nº4 (1964) - *in Russian*

[7] V.A. Kuzminsky, Matrix numerical method of stability calculation of three-dimensional boundary layers. *Uchenye Zapiski TsAGI*. **Vol. 38**, nº 3-4, pp.44-56 (2007) - *in Russian*

[8] V.D. Bokser, V.Ph. Babuev, A.Ph. Kiselev, V.G. Mikeladze and G.K.Shapovalov, The experimental investigation of HLFC-system use on the swept wing at subsonic velocities. *1997 World Aviation Congress*. Anaheim. CA. Oct. 13-16. Paper nº975500, (1997)

[9] V.A. Kuzminsky, Stability of boundary layer on swept wing with discrete suction. *Uchenye Zapiski TsAGI*. **Vol.** 37, nº3, pp.3-9 (2006) - *in Russian*

[10] A.M. Tumin and A.V. Fedorov, On the evaluation of the effect of weak flow non-uniformity in boundary layer on its stability. *Uchenye Zapiski TsAGI*. **Vol.** 13, nº6 (1982) - *in Russian*

[11] Yu.S. Kachanov and V.Ya. Levchenko, The resonant interaction of disturbances at laminar-turbulent transition in a boundary layer. *J. Fluid Mech.*. **Vol.** 138, pp.209-247 (1984)

[12] H. Deyhle and H. Bippes, Disturbance growth in an unstable three-dimensional boundary layer and its dependence on environmental conditions. *J. Fluid Mech.* **Vol.** 316, pp73-113 (1996)